Published in final edited form as:
Adv Robot. 2011 January 1; 25(15): 1879–1901. doi:10.1163/016918611X588907.

Stroke Survivors' Gait Adaptations to a Powered Ankle Foot Orthosis

Jeffrey Ward,
Arizona State University; Tempe, Arizona 85281

Thomas Sugar,
Arizona State University; Tempe, Arizona 85281

Alexander Boehler,
Arizona State University; Tempe, Arizona 85281

John Standeven, and
Washington University; Saint Louis, Missouri 63130

Jack R. Engsberg
Washington University; Saint Louis, Missouri 63130

Jeffrey Ward: Jeffrey.A.Ward@asu.edu; Thomas Sugar: Thomas.Sugar@asu.edu; Alexander Boehler: aboehler@asu.edu; John Standeven: standevenj@wusm.wustl.edu; Jack R. Engsberg: engsbergj@wusm.wustl.edu

Abstract

Background and Purpose—Stroke is the leading cause of long term disability in the United States, and for many it causes loss of gait function. The purpose of this research is to examine stroke survivors' gait adaptations to training on the Powered Ankle Foot Orthosis (PAFO). Of particular interest is the stroke survivors' ability to learn how to store and release energy properly while using the device. The PAFO utilizes robotic tendon technology and supports motion with a single degree of freedom, ankle rotation in the sagittal plane. This actuator comprises a motor and series spring. The user interacts with the output side of the spring while the robot controls the input side of the spring such that typical able body ankle moments would be generated, assuming able body ankle kinematics are seen at the output side of the spring.

Methods—Three individuals post-stroke participated in a three week training protocol. Outcome measures (temporal, kinematic, and kinetic) were derived from robot sensors and recorded for every step. These data are used to evaluate each stroke survivor's adaptations to robotic gait assistance. The robot was worn only on the paretic ankle. For validation of the kinematic results, motion capture data were collected on the third subject.

Results—All subjects showed increased cadence, ankle range of motion, and power generation capabilities. Additionally, all subjects were able to achieve a larger power output than power input from the robot. Motion capture data collected from subject three validated the robot sensor kinematic data on the affected side, but also demonstrated an unexpected gait adaptation on the unaffected ankle.

Conclusions—Sensors on the gait assisting robot provide large volumes of valuable information on how gait parameters change over time. We have developed key gait evaluation metrics based on the available robot sensor information that may be useful to future researchers. All subjects adapted their gait to the robotic assistance, and many of their key metrics moved closer to typical able body values. This suggests that each subject learned to utilize the assistive moments generated by the robot, despite having no predefined ankle trajectory input from the robot. The security of being harnessed on the treadmill led to more dramatic and favorable results.

Keywords

robotic; orthosis; ankle; gait; stroke

1 Introduction

According to the American Heart Association and the U.S. Department of Health and Human Services, each year nearly 800,000 people suffer a stroke in the United States, making it the leading cause of serious long-term disability and the third leading cause of death [1, 2]. This figure is expected to more than double within the next 50 years. This prediction is based on the elderly population growth rate that is 35 times faster than the general population, the explosion in the number of obese adults in the United States, and advances in medicine causing an increase in stroke survival rate [2, 3, 4, 5].

The adverse financial and social conditions attributed to stroke have prompted researchers and entrepreneurs to explore the viability of rehabilitation robotics. Gait therapy is a natural place to start as statistics show that post-stroke, only 33% of stroke survivors are able to achieve unassisted gait [6]. Of those patients with initial paralysis, only 10% regain functional independence [7]. These alarming statistics justify the need for rehabilitation and assistive devices, and techniques that are highly effective in aiding patients to overcome the ill effects of stroke.

Over the past decade there have been many advances in gait rehabilitation robotics with mixed results in functional benefits for the subjects [8, 9, 10, 11]. Despite these mixed results robots continue to play a multifaceted role in rehabilitation. They aid in repetitive motion tasks and allow for the application of unique force fields in the training environment that help advance our knowledge of human motor control [12]. As knowledge of human motor control expands so do the unique training algorithms of rehabilitation robots [13, 14].

A robotic gait assistance device directly and immediately addresses the mobility challenge of stroke survivors, while providing the unique ability to continuously collect important data during use. The goal of this case study is to examine stroke survivors' gait adaptations to training on the Powered Ankle Foot Orthosis (PAFO). This is accomplished by deriving gait temporal, kinematic, and kinetic key metrics from robot sensor data, recorded at 1000 Hz during every step. Section 2 will briefly discuss background on the robot. Section 3 will describe the training procedures, subsection 3.1 will describe able body robot sensor data in detail, and subsection 3.2 will illustrate how the key performance metrics are determined from the robot sensor data. Robot comfort and robustness will be discussed along with gait data collected during the three weeks of training in section 4. Subsection 4.1 will focus on the results of subjects one and two because they used a previous version of the PAFO that was scalable for multiple users, and it did not perform as well as the custom built PAFO. The data from subject three will be discussed in two subsections, 4.2 and 4.3 for robot sensor data and motion capture data respectively. Motion capture data collected from subject three are used to validate the robot sensor kinematic results.

2 Robot Background

Differences in gait for persons with stroke have been well documented in literature. The differences are characterized by slower walking speeds, greater proportion of the gait cycle occupied by the stance phase in both legs, a longer stance phase on the unaffected side, and a decrease in joint range of motion especially in the ankle plan-tarflexion during push off and knee flexion during swing phase [15]. In normal gait, the hip and knee extensors dominate the first 1/3 of the stance phase with the ankle plantarflexors dominating the last 2/3 [16]. In persons with stroke, the low level of support from the plantarflexors is compensated with knee extensors much later in stance. Hip extensors also provide greater support than normal during the first half of the stance phase [15, 16].

The PAFO developed for this study, figure 1, comprises an ankle foot orthosis with a posterior attached robotic tendon actuator (DC motor coupled to a lead-screw and lead-nut with a series spring), 9 cm lever arms, and multiple sensors; a force sensing resistor in the heel of the device, a motor encoder, and an absolute encoder at the ankle joint. The ankle encoder is solely used for data collection purposes and evaluation of key metrics. As the PAFO user’s shank rotates over the ankle joint during the loading phase of gait, the robotic tendon drives a lead-nut upward, effectively storing energy into springs. At the same time, the user’s dorsiflexion also acts to stretch and add additional energy to the springs of the robotic tendon. This control strategy has the benefit of encouraging the user to adapt his gait to more closely match the methods of storing and releasing energy seen in able-bodied gait. This is accomplished by controlling the input side of a motor series spring actuator, the robotic tendon [17, 18, 19]. Our strategy mainly differs from other impedance controlled robotic ankle devices [20], in the fact that we do not control the ankle joint. The PAFO translates a spring at the correct timing so that as a person steps and the leg rolls over the ankle, the spring stores energy that can be used at push off.

The PAFO was developed with a single degree of freedom, ankle rotation in the sagittal plane. Closed-loop (PD) control commands are derived from position feedback on the input side of the spring, while the output side is open-loop. The reference pattern for the proximal side of the spring is generated such that the elastic elements are stretched at the proper time to produce the desired ankle moment pattern [21]. In other words, the position reference command for the input side of the robotic tendon actuator is derived from typical able body ankle moments that would be generated, assuming able body ankle kinematics are seen at the output side of the spring. The controller gains are fixed and were designed using root-locust techniques on the PAFO system’s transfer function, modeled in [17]. A 1” square surface area force sensing resistor in the heel of the PAFO allows for foot strike detection even when the subject lands with a flat foot. This gait event triggers the next actuator reference pattern, which is scaled by stride time. The previous stride time is used to predict the future stride timing. Because the subjects walked at a relatively constant pace in a controlled environment, this strategy worked quite well.

Gait assistance is provided at a 50% level from the robot. This is achieved by calculating a motor pattern that would provide a full ankle moment, assuming the same able body ankle kinematics, to a user with half the body weight. A major challenge of developing a custom fit PAFO was integrating the motor, lever arms, and sensors to the polypropylene copolymer orthosis. Details of the design can be seen in figure 1. For more detail on the design and previous control strategies of this robot see the following reference [17].

Other naturally compliant wearable devices include a pneumatically actuated lower limb orthosis developed at University of Michigan, and a robotic ankle foot orthosis powered by a series elastic actuator developed at MIT [22, 20]. The MIT variable impedance ankle foot orthosis has been shown to reduce the number of foot slaps and increase the amount of dorsiflexion degrees during the swing phase in two stroke survivors [20]. While their device adequately addressed two of the common gait deficiencies of stroke survivors (foot-slap and toe-drag), our approach addresses the lack of push off power at the ankle while ensuring enough assistive moment for toe clearance in the swing phase. Supplementing the push off power at the ankle will directly affect the previously mentioned compensation mechanisms of stroke gait.

Healthy humans have shown an ability to quickly adapt their gait to an active ankle foot orthoses developed at the University of Michigan. Their research shows that the type of control algorithm greatly influences the quality and degree of adaptation. Proportional myoelectric control produced more natural gait kinematics as opposed to a forefoot triggered plantarflexion assist control mode [23]. Those results suggest that allowing for a more graded response in orthosis dynamics along with providing a control mode that is similar to the normal physiological control modes allow for the return of normal kinematic patterns for healthy subjects after only a short training period on an active ankle foot orthosis. However, implementing myoelectric control into a wearable robot for stroke therapy, especially a gait robot, would be problematic. Stroke survivors have difficulty generating the efferent signals for muscle contraction. The PAFO does not implement myoelectric control and no physiological control modes are assumed for a stroke survivor, due to their neurological injury. However, the PAFO does allow stroke survivors to uniquely adapt their gait to an assistive moment. This approach has demonstrated some interesting results, discussed in section 4.

Multiple degrees of freedom systems that attempt to accommodate the complex motions of the ankle joint have also been explored [24, 25, 26, 27]. Alternative approaches include base mounted, non-wearable and strictly therapeutic systems like the Lokomat and Haptic walker. These are large, direct drive systems that simulate compliance through complex control algorithms [28, 29]. Another base mounted therapy robot developed at the University of Delaware utilizes a force field controller to accomplish an “assist-as-needed” therapy strategy that has shown great promise in the rehabilitation of stroke survivors [30].

3 Subject Testing Methods

To truly evaluate the effectiveness of the PAFO as an assistive device, stroke subjects must use the device while kinematic and kinetic data are collected. This protocol involves two components, training and testing. The research protocol was approved by the IRB at Washington University in St. Louis where the testing was performed. See table 1 for details of the subjects that have participated in this study. Key inclusion criteria included being able to: stand independently for two minutes, move from sit to stand, walk 7 meters 10–15 times with rest, demonstrate adequate motion of the lower limb joints, and follow simple commands. Subjects were allowed to use their normal walking aids if necessary during the assessment and testing only when the PAFO was not worn. No subject used additional walking aids while the PAFO was donned. Key exclusion criteria included any serious medical condition and excessive pain.

All subjects trained three times per week for three consecutive weeks. The training session consisted of five components: 1) warm-up (five minutes), 2) over ground gait pre (six minutes), 3) treadmill gait (twelve minutes), 4) over ground gait post (six minutes), and 5) cool-down (five minutes). During warm-up and cool-down, the subjects performed some light stretching mainly focused on the lower extremities (calves, hamstrings, and quadriceps). The actual treadmill training with the PAFO focused on improvement in gait kinematics and increasing gait speed and duration. Sensor data from the robot was logged at 1000 Hz for the middle three minutes of components 2 and 4, and for the middle six minutes of component 3. The number of steps recorded for each three minute period was between 65 and 145 depending on subject gait speed. For the custom built robot, over 85% of these steps were used in evaluating the key ankle gait metrics.

The testing component for the motion capture data collected on subject three involved a gait analysis outcome test which occurred during two sessions (pre- and post-training), when the subject wore the PAFO. Kinematic data were collected from both sessions with a motion capture system at a rate of 60 Hz. Three surface markers were placed on the trunk, pelvis, thighs, legs, and feet in a standardized method [31]. For each session the subject was asked to walk at their freely chosen walking speed along a fifteen meter walkway and had data collected during the middle two meters. Six to eight trials of data were collected, resulting in twelve to fifteen complete gait cycles that were used to produce average curves. Motion capture analysis produced averaged lower limb sagittal plane kinematics for subject three.

The primary source of data came from the sensors on the robot. These data were recorded during training and for each step during the three week period for all subjects. The robot measures the deflection of the spring to calculate the force applied by the robot to the ankle, measures ankle angle from an absolute encoder, determines heel strike from a force sensing resister, and records the angular velocity of the shank from a rate gyro. From these sensors, key gait evaluation metrics were determined. Statistical analyses (means, standard deviations, and t-tests) were performed on key variables for each individual subject to determine if the means of each variable had changed over the course of their training.

3.1 Able Bodied Gait Data from the PAFO

The graph of figure 2(a) shows kinematic data taken directly from the absolute encoder of the PAFO which measures the ankle joint motion in the sagittal plane. Note that “lever position” in the legend, also known as ankle displacement, is analogous to ankle angle. The lever position is a measure of vertical displacement referenced from the zero position of the absolute encoder at the ankle, which is the anatomical position, the foot being perpendicular to the tibia.

$$LeverPosition = LeverArm \cdot AnkleAng(rad)$$

The sine term is eliminated for simplicity with insignificant errors to the lever position calculation due to the small maximum range of motion at the ankle for our stroke survivor subjects (20 degrees). When the dark black line is above zero, this corresponds to dorsiflexion, and below zero corresponds to plantarflexion. When the dark black line is at zero, this means the foot is perpendicular to the shank.

The dashed blue line in figure 2(a) is the reference command for the actuator nut position, and the solid red line is the actual nut position. Because of the controller gains, the red line always closely follows the blue line. Negative nut position means the nut is moving upward, which stretches the springs tending to plantarflex the foot.

Unlike impedance controlled ankle devices that modulate their controller based on the ankle position, the PAFO applies a motor pattern that would provide an able body ankle moment if the device user matches able body ankle kinematics. This allows the user to store as much energy into the springs of the robotic tendon as possible, but does not mandate an ankle trajectory. Notice in the shaded area above zero millimeters the user’s position exerts a positive stretch on the springs, while the nut also positively stretches the springs. Also, notice that the user has a large range of lever arm displacement (−20mm to 8mm). This able bodied user is adding a significant amount of energy to the system by “stepping through” each cycle. The spring is being deflected in the shaded area storing and then releasing energy.

The able bodied subject has good power amplification by releasing the combined (human - motor) stored energy at a swift rate, figure 2(b). The relationship between the slopes of the nut displacement and lever displacement curves directly determine the input and output mechanical power respectively, figure 2. These slopes and the power curves provide insight into the power supplied by the user as opposed to the motor alone.

3.2 Key Performance Metrics Defined for PAFO Sensor Data

There are a total of 11 key metrics that will be examined for each subject training with the PAFO. These variables were recorded for every “good” step and evaluated on a daily basis. A “good” step is defined as a step that has no robot abnormalities. For example, the previously designed and scalable robot would frequently miss the heel strike signals. The result of a missed heel strike signal is that the robot will only function as a passive device for that step. This would be viewed as a “bad” step and the data for that step would not be included into the variable statistics. There are 12 variables listed below, the 11 key variables and an extra variable, stride length, calculated for subject three from known treadmill speed and cadence. The means and standard deviations are recorded for each variable over the total steps taken per day. Beginning with subject three, the first subject to use the custom PAFO, these data are divided by day and also by whether the subject walked over ground or on the treadmill. Figure 3(a) shows the ankle displacement and motor pattern. Notice the black and red dots indicate maximum dorsiflexion and plantarflexion respectively. The gray colored dashed lines intersect with the vertical and horizontal axes of each graph to highlight the value of the variable and the gait % at which that value occurs. See figures 3(b) and 3(c) for the moment metrics and power metrics respectively.

- Key Performance Metrics

    1. Cadence (steps/min)
    2. Maximum Dorsiflexion (mm)
    3. Gait % at Maximum Dorsiflexion (%)
    4. Maximum Plantarflexion (mm)
    5. Gait % at Maximum Plantarflexion (%)
    6. Range of Motion (mm)
    7. Maximum Moment (Nm)
    8. Gait % at Maximum Moment (%)
    9. Mechanical Power Output (Watts)
    10. Gait % at Maximum Power Output (%)
    11. Power Amplification (Power Out/Power In)
    12. Stride Length (m)

4 Results and Discussion

4.1 Robotic Gait Data Results - Subjects One and Two

The robot data collected and presented here indicates both a measure of robot performance as well as subject adaptability to robotic gait influences. The first two subjects used the previously designed scalable PAFO. For this reason, their performance will be evaluated separately from the third subject. Due to the mechanical structure of the scalable robot, both subjects wore foam padding under the shoe of their unaffected leg to even the height of both feet. Additionally, the foot-bed was made of rigid plastic and only extended to the end of the metatarsals, just before the proximal phalanges. These facts led to a performance reduction in all key metrics as well as increased variability when compared with the third subject. Despite the limitations of the previous robot, some noteworthy results were recorded. Each key metric was recorded for every step on a given trial day. The mean and standard deviation for these metrics were calculated. For accurate comparison, only days that had at least twenty good data points, or steps, were used. Otherwise, the data for that day were rejected. Table 2 summarizes the results of all key metrics for the first subject.

In table 2, notice the reduction in the standard deviation for all variables except peak power output where the increase in the standard deviation was very slight. This suggests that the subject became more comfortable wearing the robot as her measured gait variables became more consistent. The significant findings from the table, as highlighted by the 1 in the "t-test" column, are:

1. Mean cadence increased by 12%, from 24.1 steps/min to 27 steps/min.
2. Positive dorsiflexion values were achieved, going from −0.9mm early in the study to 1.4mm by the end.
3. Range of Motion increased 3.2 mm (57%) or 2 degrees.
4. Maximum Moment showed a significant 20% improvement going from 16.3 Nm to 19.5 Nm with reduced variability.
5. Mean Peak Power out increased 89%, from 7.5 Watts to 14.2 Watts.

The increased dorsiflexion primarily contributed to the increase in overall range of motion for subject one, which suggests that by the end of the study she was able to store more energy in the robot's elastic elements. This idea is supported by the increases in peak moment and peak power out. The amplitude increase in peak moment is only partly attributed to an increase in gait speed, higher moments are required at faster speeds, as our first subject increased her speed by 12% while her ankle moment increased by 20%. While this is encouraging, the peak power out values are still very low. This is primarily attributed to slow walking, which requires much less power. Despite the low power values, the first subject was able to increase her gait power by an impressive 89%.

Figure 4 (A) demonstrates the kinematics, (B) the ankle moment, and (C) the power of a typical step early in the training (left) and late in the training (right) for subject one. The dashed line intersects zero ankle moment. Typically this should occur at toe-off, or peak plantarflexion. Notice that early in the study the subject has an early toe-off and is resisting the supplied moment from the robot. Toward the end of training the zero moment and toe-off line up, suggesting that the subject has adapted her gait to take advantage of the robot assistance. This conclusion is further supported by the increased power amplification late in the study, shown at the bottom of figure 4.

Refer to table 1 for a description of subject two, and table 3 for a list of his key metric values. There are also many significant changes in the second subject's key metrics:

1. The standard deviation of maximum dorsiflexion, % gait at maximum dorsiflexion, % gait at maximum plantarflexion, peak moment, and % of gait at peak power all showed reduction.
2. Mean cadence increased by 12.5%, going from 35.2 steps/min to 39.6 steps/min.
3. Max dorsiflexion dropped from −2.5 mm to −3.7 mm, or a total of 0.76 degrees.
4. Max plantarflexion changed from −6.4 mm to −21 mm, a 228% increase (9.3 degrees) in amplitude.
5. Range of motion increased by 338%, or 13.2 mm correlating to 8.4 degrees.
6. Peak moment decreased by 45%, going from 31.8 Nm to 17.4 Nm.
7. % gait at peak moment showed a significant change from 64.9% to 51.3%.

8. % gait at peak power reduced 4.9% to a value of 56.3%.
9. Power amplification ratio grew by 115%, going from 0.7 to 1.5.

For subject two, the overall range of ankle motion increased, primarily due to a large increase in plantarflexion amplitude (dorsiflexion was reduced). Additionally, despite no significant change in maximum ankle moment or output power, the user's power amplification significantly increased to 1.5. This was accompanied by a reduction in % gait at peak moment. The % gait at peak moment is trending toward able bodied results. These facts suggest that the percent contribution of power from the user increased throughout the study.

Both subjects used the previously designed and scalable robot that was plagued with fit and performance issues. Although there were some variables that indicate decay, there are others that indicate improvement. Both subjects increased their gait speed while wearing the PAFO.

4.2 Robotic Gait Data Results - Subject Three

Subject three was the first user of the custom fit PAFO shown in figure 1(b). There are advantages of using a custom robot over a one size fits all device. First, a more comfortable and secure fit will improve device acceptance and performance. Second, a flexible foot-bed allows a more natural progression of the center of pressure on the foot as opposed to a rigid plastic foot-bed. Additionally, the foot-bed height matches the height of the subject's normal shoes worn during training (increases subject stability), and the custom fit allows for more uniform loads on the subject as the robot is not deforming around the shank. These benefits led to an increased stability of the subject. The following data are broken into treadmill testing, and over ground testing. The subject's performance was markedly different under each condition, which could be expected as the experience for the user is different. While on the treadmill the subject has the comfort of knowing he's protected from a fall with a harness, and has a rail that he can hold onto if he begins to feel unstable. Table 4 shows the pre- and post-results for all the key metrics for over ground walking while table 5 lists these results for treadmill walking.

For over ground data, cadence had a slight (6.6%) increase of 2.3 steps/min over the course of the entire study. These data demonstrated an upward stair stepping trend at a slow but consistent rate. In contrast, the treadmill data shows a dramatic jump in steps/min on the seventh day, and continues to increase steadily for the remainder of the study, figure 5(a). This is the likely result of the confidence the subject had while being harnessed on the treadmill. Additionally, stride length was calculated for subject three from the cadence and known treadmill speed. Subject three increased his stride length by 50% to 0.82 meters. This result was aggressively trending toward the "typical value" of 1 meter, figure 5(b).

The affected ankle kinematics for the third subject improved, according to the robot sensor data collected during the study. During over ground gait, no significant change was observed in maximum dorsiflexion. Examining the graph of figure 6 shows that the dorsiflexion for over ground data are much more variable than treadmill data. Additionally, on the last day of testing the subject's maximum dorsiflexion values dropped significantly from the previous 4 days. However, a 28% increase in maximum plantarflexion was observed. This put the subject's plan-tarflexion values on par with "typical values" seen for this metric. The results led to an overall range of motion increase of 32% or 5 millimeters (3.2 degrees) for over ground data. See figure 6 for a series of three graphs on ankle kinematics; maximum dorsiflexion, maximum plantarflexion, and range of motion plotted for over ground and treadmill data.

For treadmill data the results were again more dramatic. The subject improved all kinematic parameters, maximum dorsiflexion grew to 11.5 millimeters while plantarflexion amplitude grew to 19.2mm, increasing the ankle range of motion by 48%, achieving near "typical values" seen by other able bodied users of the PAFO.

Ankle kinetic data demonstrated very different results for over ground versus treadmill. The over ground data showed significant change only in peak moment, which was decreased by 1.6 Newton meters. Figure 7 shows three graphs; peak moment, peak power, and power amplification for over ground and treadmill data. It should be noted that peak power and moment data had a significant drop on the last day of training, as compared with the day before. If the prior day was considered the last day of the study, significant increases would have been seen in both variables. The cause for this drop on the last day of training are unknown. The over ground data are typically more variable than the treadmill data, figure 7.

In contrast, the treadmill results were very positive. The peak moment increased by 37%, or 10 Newton meters. The peak power increased by 89%, or 23.6 Watts. Power amplification measured 2.4 on the 22nd day,

The over ground data for both gait % at maximum dorsiflexion and plantarflexion are highly variable. T-test analysis shows that the 1.8% reduction in gait % at maximum dorsiflexion is significant. Gait % at which maximum dorsiflexion occurs moved toward "typical values" but the gait % at maximum plantarflexion remained constant. For treadmill data both variables were significant, with gait % at maximum dorsiflexion moving 6% closer to "typical values," but gait % at maximum plantarflexion moving away from "typical values" by 1.3%.

The timing for peak moment and peak power improved in both the over ground and treadmill case. The over ground case had much higher variability, but still showed significant reductions in gait % at peak power and moment occurrence. These values trended toward "typical values." Again, the timing for the treadmill case was closer to "typical values" than the over ground case. As discussed in pathological gait research, stroke survivors typically have delayed moment and power generation [15].

4.3 Motion Capture Comparison with Robot Data for Subject Three

Motion capture data for both the affected and unaffected ankles were collected while subject three wore the PAFO over ground. Eight trials of data were collected and averaged pre- and post-training to generate the graphs in figure 8. Figure 8(a) illustrates the ankle angles pre- and post-training for the right, affected side, donned with the PAFO. These results agree with the previously reported results derived from robot data; a large increase in plantarflexion was achieved post-training; no change in maximum dorsiflexion was observed; however, the 8 degrees of dorsiflexion obtained is similar to able bodied values. The pre-training ankle angle motion capture data for the right leg show zero plantarflexion. Subject three is resisting the forces generated by the robot during the initial training session; however, by the post-training assessment his range of motion has increased.

According to the motion capture data, gait adaptation has also occurred on the left, unaffected side. Figure 8(b) highlights the left, unaffected, ankle angles pre- and post-training. Ankle angles on the left side show a very late toe off (85% of gait), along with an uncharacteristic drop in dorsiflexion between 16% and 64% of gait. Stroke survivor gait typically has a very late toe off on the unaffected side. However, the drop in dorsiflexion of the unaffected leg between mid-stance and mid-swing is caused by a rising heel on the unaffected side. This behavior can be seen in pre-training motion capture data collected without utilizing the PAFO, but is amplified when the PAFO is employed. Subject three has an interesting left leg adaptation to the forces and powers applied to his right leg. See figure 9 for an illustration of subject three raising his heel during a gait cycle. The picture sequences from left to right, and top to bottom. From the picture in figure 9 it can be seen that slightly before toe off of the affected ankle, just before peak power is transferred from the robot, the heel on his unaffected leg begins to rise. Rising of the left heel continues until “feet adjacent,” which signals mid-swing of the right leg. At mid-swing of the right leg, the left heel begins dropping in preparation for its abbreviated loading phase and toe off. It appears from these data and illustration that subject three is slightly hopping over the power spike provided by the PAFO. This is most likely due to lack of knee strength, and to prevent hyperextension. Another explanation comes from research in pathological gait that has shown that fast walkers in the stroke group demonstrate large

5 Conclusion

The robotic tendon actuator allowed for the development of a lightweight and compliant gait assisting device. This research has developed a set of key metrics derived from sensors on the robot. These metrics provide a useful and effective means of examining important gait kinematic, kinetic, and timing parameters. This information could be used to improve device performance, monitor the health of the subject by looking for gait anomalies, and potentially to even guide clinicians on tailoring a therapy program to a specific user.

Comfort, stability, and robustness proved to be critical design parameters for developing a gait assisting robot capable of collecting repeatable data with low variability. For example, a flexible foot-bed allowed for a more natural progression of the center of pressure on the foot as opposed to a rigid plastic foot-bed. With the custom device, the foot-bed height matched the height of the subject’s normal shoes worn during training and increased his stability. Additionally, the custom fit allows for more uniform loads on the subject as the robot is not deforming around the shank, and the ankle joints between subject and robot are more closely aligned. Misalignment of the ankle joints causes relative motion between robot and user. A custom robot requires fewer adjustment mechanisms which improve reliability.

NIH-PA Author Manuscript

NIH-PA Author Manuscript

All stroke survivors adapted to the robot and were able to use it to enhance push off power. Over the course of the training, many of their key ankle gait metrics moved closer to typical able body values. This is remarkable when considering that no predefined ankle trajectory is defined by the robot, as it only controls the input side of the spring. All subjects successfully learned to properly store and release energy while using the PAFO, as demonstrated by their significant power amplification factor and increased ankle range of motion. Subjects one and three also increased output power and moment. Subject three was able to adapt his gait to the robot very effectively while on the treadmill. His data stands out from subjects one and two primarily because of the custom fit robot. Key metric changes were more dramatic while harnessed and using a treadmill. Over ground robot data suggests that positive changes in gait variables do occur, but at a slower rate than while on the treadmill.

The data for subject three had a significant change for every key metric from the treadmill data. For the over ground data there were 7 of the 11 variables that had a significant change. While on the treadmill, 9 of 11 key metrics showed improvement, suggesting that the subject was able to adapt his gait and utilize the power supplied for push off from the robot. Separate motion capture data analysis confirms the results from the analysis of the robot sensor data for the paretic ankle. Additionally, the motion capture data highlights a unique gait adaptation on the unaffected side of subject three, characterized by a rising of the left (unaffected) heel during PAFO power generation on the affected ankle. This adaptation could result from an attempt to augment "pull-off" powers from the affected hip flexors, or to prevent knee hyperextension due to weak knee muscles. We found that high level stroke survivors are more capable of supporting augmented ankle power through the knee joint.

These positive results provide strong support for future work and the data collected in this study will aid in determining the required number of subjects for a clinical trial. This clinical trial will include a placebo therapy to distinctly determine the effects of robotic gait assistance on over ground unassisted gait. Due to the unaffected side gait adaptations of subject three, two PAFO systems may be utilized and both legs monitored.

Acknowledgments

This work was supported by the National Institutes of Health

References

1. Lloyd-Jones D, Adams R, Brown T, Carnethon M, Dai S, De Simone G, Ferguson T, Ford E, Furie K, Gillespie C, et al. Heart disease and stroke statistics–2010 update. A report from the American Heart Association. Circulation. 2009
2. Health, united states, with chartbook on trends in the health of americans. 2006
3. Taub E. Guest editorial: New discovery equals change in clinical practice. Journal of Rehabilitation Research and Development. 1999; 36(3):vii–viii. [PubMed: 10659797]
4. Agrawal SK, Erdman AG. Biomedical assist devices and new biomimetic machines-a short perspective. Journal of Mechanical Design. 2000; 127:799–800.
5. Kurth T, Gaziano JM, Berger K, Kase CS, Rexrode KM, Cook NR, Buring JE, Manson JE. Body mass index and the risk of stroke in men. Arch Intern Med. 2002; 162(22):2557–2562. [PubMed: 12456227]

6. Wandel, Jorgensen HS, Nakayama H, Raaschou HO, Olsen TS. Prediction of walking function in stroke patients with initial lower extremity paralysis: The copenhagen stroke. Archives of physical medicine and Rehabilitation. 2000; 81(6):736738.

7. Jorgensen HS, Nakayama H, Raaschou HO, Olsen TS. Recovery of walking function in stroke patients: The copenhagen stroke study. Archives of Physical Medicine and Rehabilitation. 1995; 76(1):27–32. [PubMed: 7811170]

8. Mirelman A, Bonato P, Deutsch J. Effects of training with a robot-virtual reality system compared with a robot alone on the gait of individuals after stroke. Stroke. 2009; 40(1):169. [PubMed: 18988916]

9. Deutsch J, Latonio J, Burdea G, Boian R. Post-stroke rehabilitation with the Rutgers Ankle System: a case study. Presence: Teleoperators & Virtual Environments. 2001; 10(4):416–430.

10. Hornby T, Campbell D, Kahn J, Demott T, Moore J, Roth H. Enhanced gait-related improvements after therapist-versus robotic-assisted locomotor training in subjects with chronic stroke: a randomized controlled study. Stroke. 2008; 39(6):1786. [PubMed: 18467648]

11. Israel J, Campbell D, Kahn J, Hornby T. Metabolic costs and muscle activity patterns during robotic-and therapist-assisted treadmill walking in individuals with incomplete spinal cord injury. Physical Therapy. 2006; 86(11):1466. [PubMed: 17079746]

12. Reinkensmeyer D, Emken J, Cramer S. Robotics, motor learning, and neurologic recovery. Biomedical Engineering. 2004; 6(1):497.

13. Emken, JL.; Bobrow, JE.; Reinkensmeyer, DJ. Robotic movement training as an optimization problem: Designing a controller that assists only as needed. Rehabilitation Robotics, 2005. ICORR 2005. 9th International Conference on; 2005. p. 307-312.

14. Reinkensmeyer, D.; Emken, J.; Liu, J.; Bobrow, J. Advances in Computational Motor Control III. San Diego, CA: 2004. The nervous system appears to minimize a weighted sum of kinematic error, force, and change in force when adapting to viscous environments during reaching and stepping. http://www.bme.jhu.edu/acmc/

15. Olney SJ, Richards C. Hemiparetic gait following stroke. part i: Characteristics. Gait and Posture. 1996; 4(2):136–148.

16. Winter, DA. The biomechanics and motor control of human gait: normal, elderly and pathological. University of Waterloo Press; 1991.

17. Ward J, Boehler A, Shin D, Hollander K, Sugar T. Control architectures for a powered ankel foot orthosis. International journal of Assistive Robotics and Mechtronics. 2008; 9(2):2–13.

18. Hollander KW, Ilg R, Sugar TG, Herring D. An efficient robotic tendon for gait assistance. J Biomech Eng. 2006; 128(5):788–91. [PubMed: 16995768]

19. Hollander, KW.; Sugar, TG. Design of the robotic tendon. Design of Medical Devices Conference (DMD 2005); 2005;

20. Blaya JA, Herr H. Adaptive control of a variable-impedance ankle-foot orthosis to assist drop-foot gait. Neural Systems and Rehabilitation Engineering, IEEE Transactions on. 2004; 12(1):24–31.

21. Hitt, J.; Oymagil, AM.; Sugar, T.; Hollander, K.; Boehler, A.; Fleeger, J. Dynamically controlled ankle-foot orthosis (dco) with regenerative kinetics: Incrementally attaining user portability. IEEE International Conference on Robotics and Automation; 2007. p. 1541-1546.

22. Gordon KE, Ferris DP. Learning to walk with a robotic ankle exoskeleton. J Biomech. 2007; 40(12):2636–44. [PubMed: 17275829]

23. Cain SM, Gordon KE, Ferris DP. Locomotor adaptation to a powered ankle-foot orthosis depends on control method. J Neuroeng Rehabil. 2007; 4:48. [PubMed: 18154649]

24. Ward J, Hitt J, Sugar T, Bharadwaj K. Dynamic pace controller for the robotic gait trainer. ASME-IDETC. 2006:7.

25. Agrawal, A.; Banala, SK.; Agrawal, SK.; Binder-Macleod, SA. Design of a two degree-of-freedom ankle-foot orthosis for robotic rehabilitation. Proceedings of IEEE International Conference on Rehabilitation Robotics (ICORR); 2005; p. 41-44.

26. Forrester LW, Roy A, Krebs HI, Macko RF. Ankle training with a robotic device improves hemiparetic gait after a stroke. Neurorehabilitation and Neural Repair. Nov.2010

27. Roy A, Krebs H, Williams D, Bever C, Forrester L, Macko R, Hogan N. Robot-aided neurorehabilitation: a novel robot for ankle rehabilitation. Robotics, IEEE Transactions on. 2009; 25(3):569–582.

28. Bernhardt M, Frey M, Colombo G, Riener R. Hybrid force-position control yields cooperative behavior of the rehabilitation robot lokomat. ICORR. 2005:536–539.

29. Schmidt, H.; Piorko, F.; Bernhardt, R.; Kruger, J.; Hesse, S. Synthesis of perturbations for gait rehabilitation robots. Proceedings of IEEE International Conference on Rehabilitation Robotics (ICORR); 2005. p. 74-77.

30. Banala SK, Kim SH, Agrawal SK, Scholz JP. Robot assisted gait training with active leg exoskeleton (ALEX). IEEE Transactions on Neural Systems and Rehabilitation Engineering. 2009; 17(1):28.

31. Engsberg JR, Lenke LG, Hollander KW, Uhrich ML, Commean PK, Lee JR, Bae KT. Methods to locate center of gravity in scoliosis. Spine. 2003; 28(23):E483–9. [PubMed: 14652482]

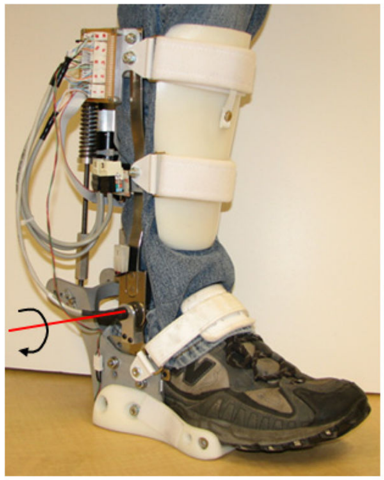
(a) Scalable PAFO

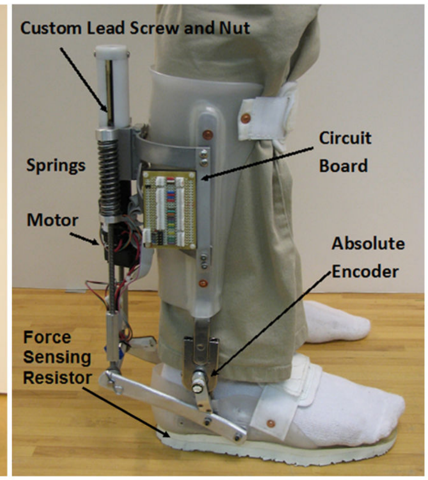

(b) Custom PAFO

Figure 1.
Scalable PAFO (a), Custom designed PAFO (b)

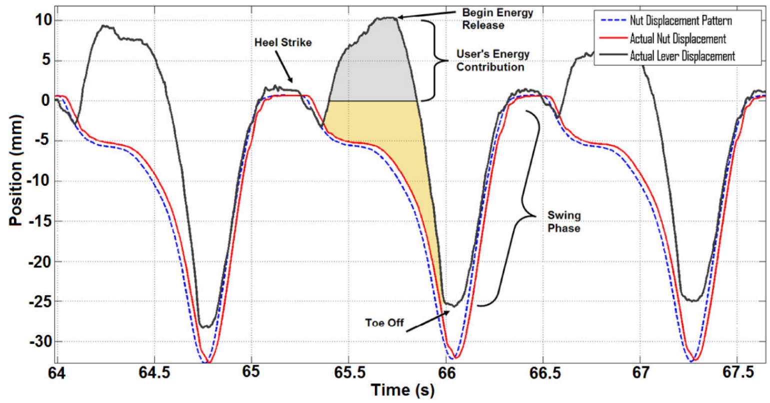

(a) Gait Kinematics

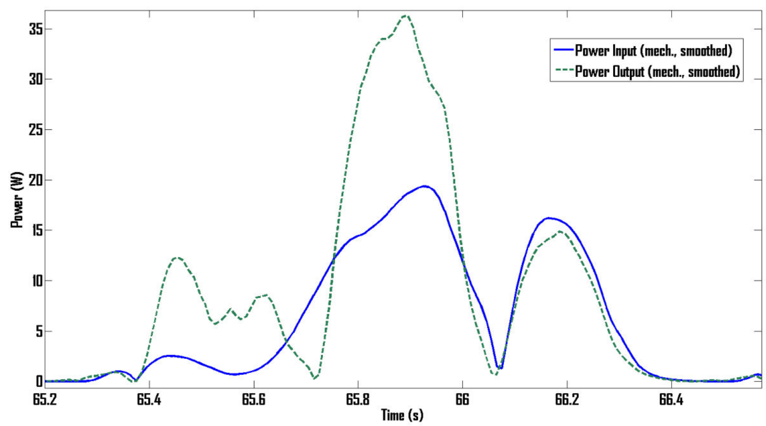

(b) Gait Power

Figure 2.

Able bodied gait data collected from the absolute encoder on the PAFO showing lever position, lead nut reference signal and actual lead nut position (a), Absolute value of ankle power data collected on the PAFO from a slow walking, 65 *kg* user (b)

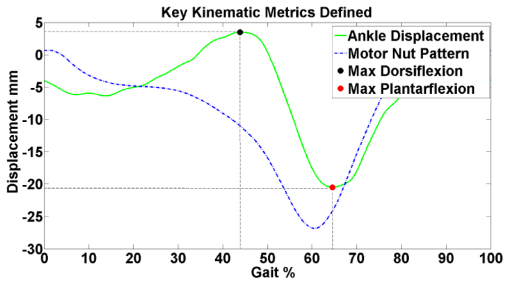

(a) Key Kinematic Metrics

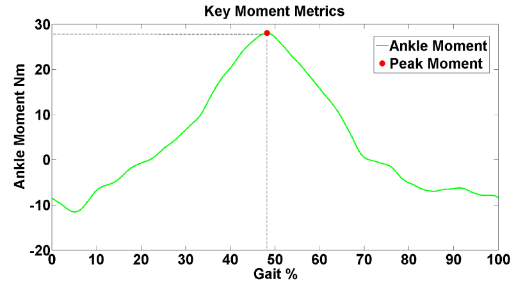

(b) Key Moment Metrics

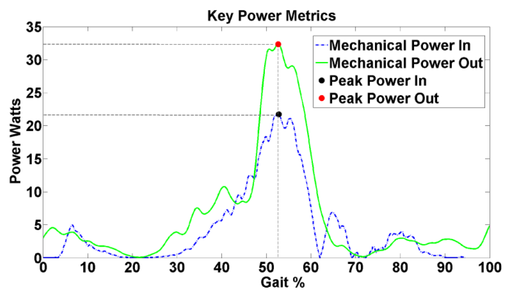

(c) Key Power Metrics

Figure 3.

Key kinematic (a), moment (b), and power (c) metrics calculated per step

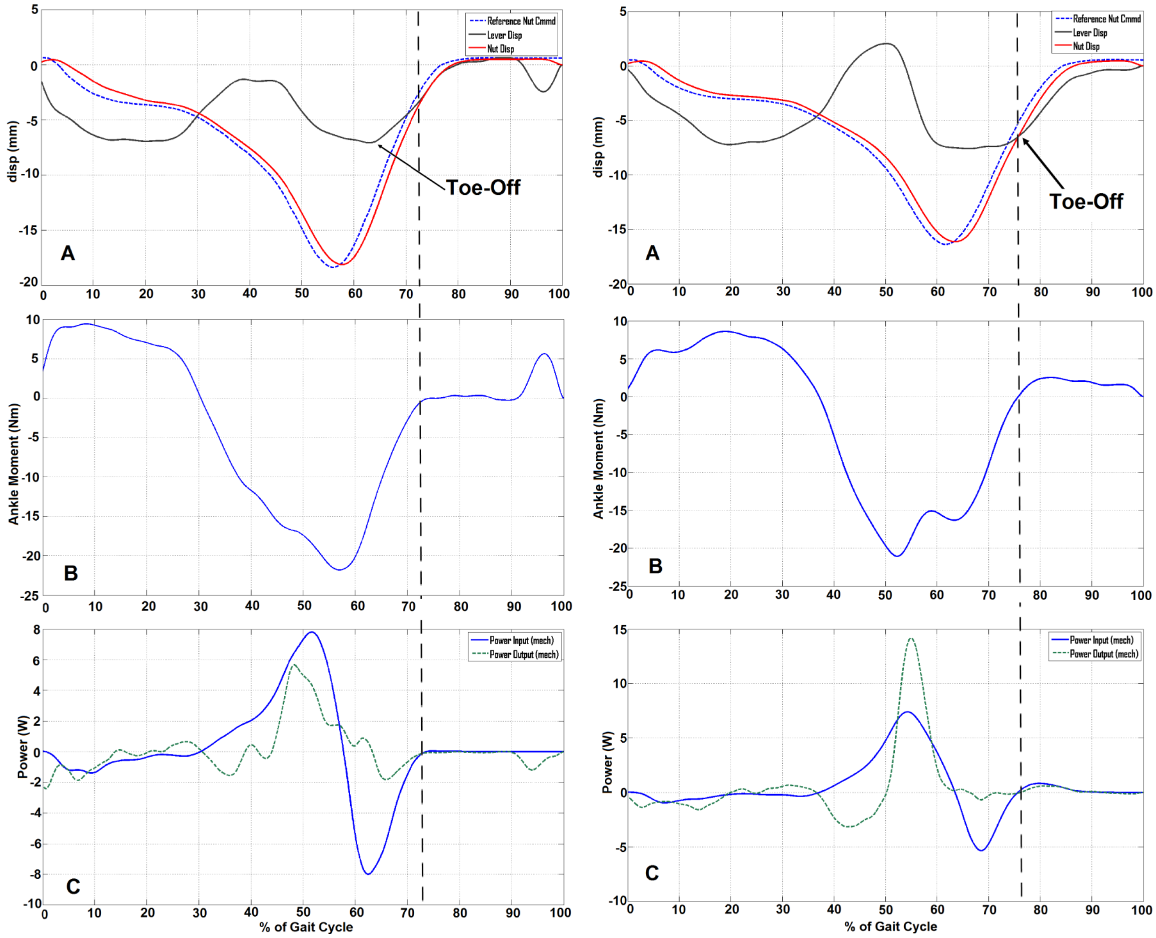

Figure 4.
Kinematic and kinetic data collected from the first stroke survivor subject early (left) and late (right) in the training, the black dashed line indicating gait % at zero ankle moment

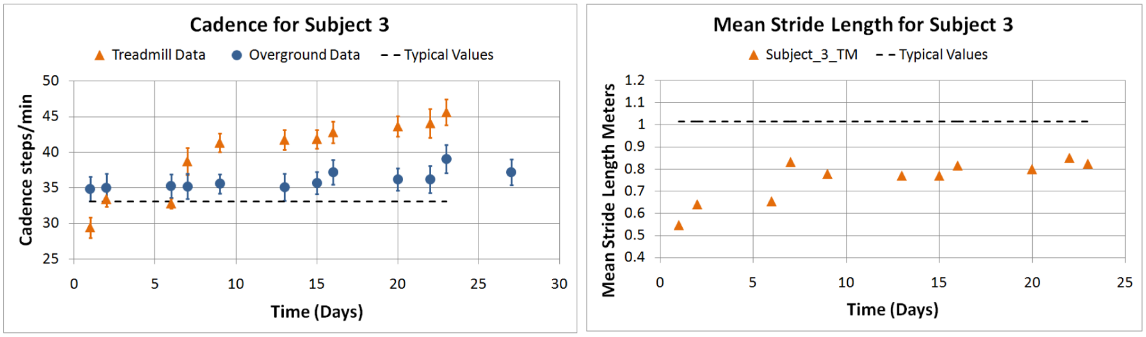

(a) Cadence (b) Mean Stride Length

Figure 5.

Treadmill and over ground cadence steps/min with error bars showing plus and minus one standard deviation (a), and calculated stride length in meters (b) for subject three

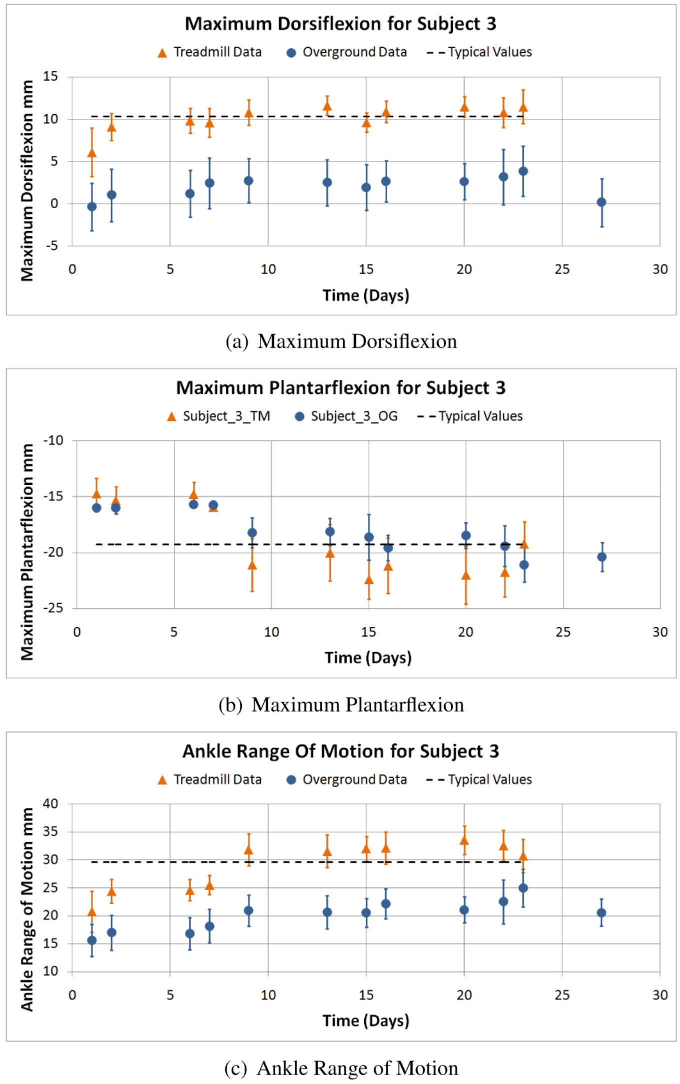

Figure 6.

Maximum dorsiflexion (a), maximum plantarflexion (b), and range of motion (c) plotted for over ground and treadmill data from subject three with error bars showing plus and minus one standard deviation

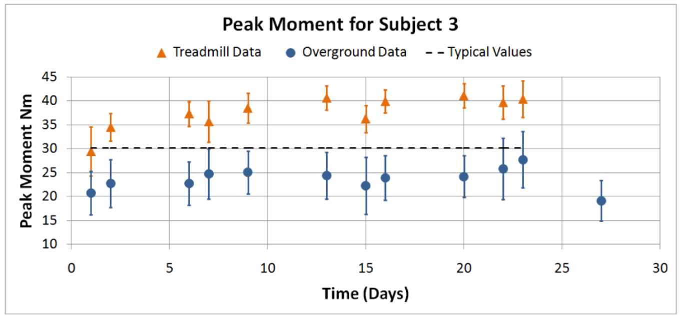

(a) Peak Moment

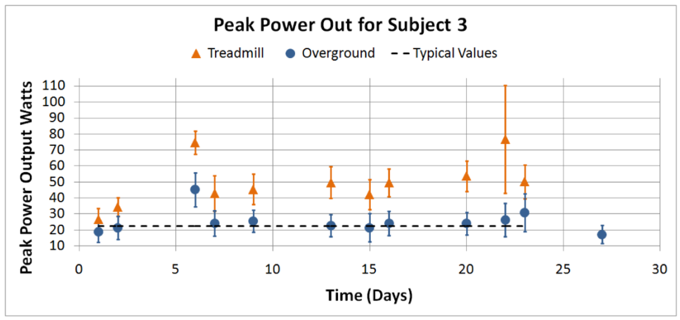

(b) Peak Power Output

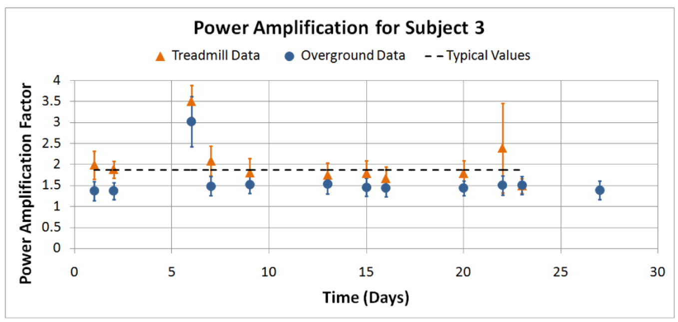

(c) Power Amplification

Figure 7.

Peak moment (a), peak power output (b), and power amplification ratio (c) plotted for over ground and treadmill data from subject three with error bars showing plus and minus one standard deviation and floated around “typical values” of 1.9 for the entire study.

NIH-PA Author Manuscript
NIH-PA Author Manuscript

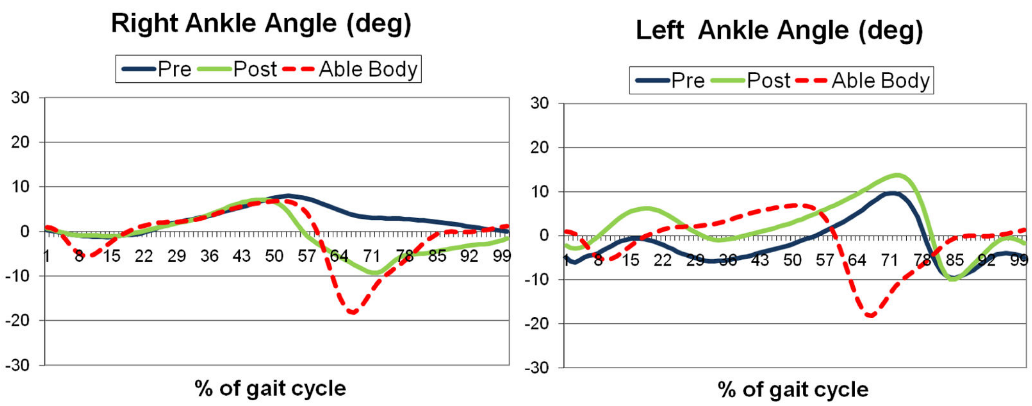

(a) Right Paretic Ankle Data

(b) Left Unaffected Ankle Data

Figure 8.

Able body ankle angle and subject three's ankle angle (degrees) collected from motion capture data while the subject is utilizing the PAFO, right affected ankle donned with PAFO (a), left unaffected ankle (b)

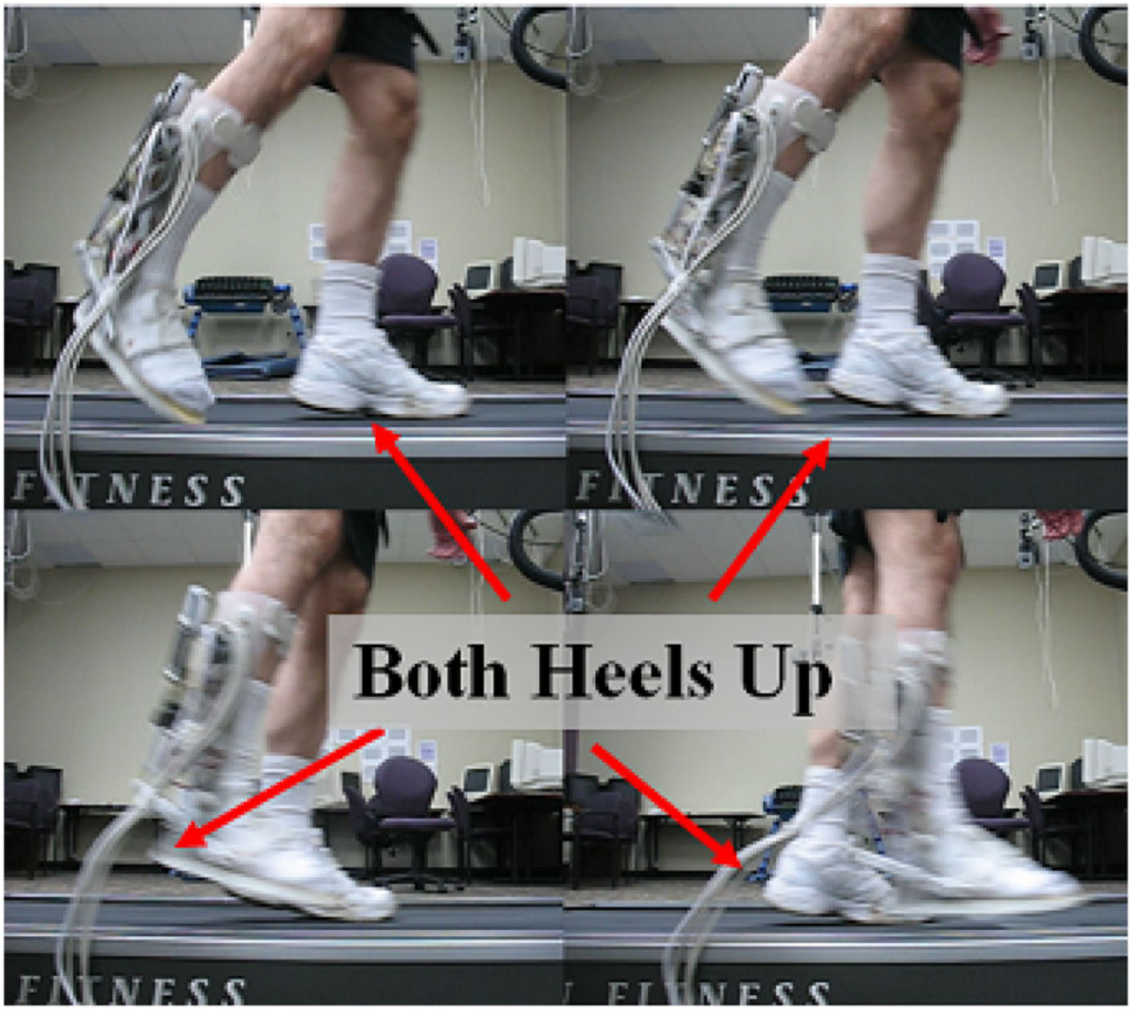

Figure 9.
Sequencing from left to right and top to bottom, the illustration shows that as subject three approaches toe off, the opposite (left) heel rises until mid swing "pull-off" powers at the hip in late stance. Raising up on the opposite heel would act to augment the "pull-off" power from the hip on the affected side [15].

NIH-PA Author Manuscript
NIH-PA Author Manuscript

Table 1

Subject Information Table

Subject #	**1**	**2**	**3**
Age (yr)	60	48	48
Sex m/f	f	m	m
Weight (kg)	81.6	93.0	79.4
Height (cm)	152	183	178
Affected Side L/R	L	L	R
# Months Post Stroke	204	240	300
Custom or Scalable PAFO C/S	S	S	C

NIH-PA Author Manuscript
NIH-PA Author Manuscript

Table 2

Subject One Key Metrics

	pre	(+/−) Std	post	(+/−) Std	Delta	t-test	Typ Val
cadence (steps/min)	24.1	0.2	27.0	0.1	2.9	1.0	33.1
Max Dorsiflexion (mm)	−0.9	1.8	1.4	1.3	2.3	1.0	10.3
Max Dorsiflexion (degrees)	−0.6	1.1	0.9	0.8	1.5	1.0	6.6
% of Gait @ Max Dorsi-	47.7	8.2	49.3	1.9	1.5	0.0	39.8
Max Plantarflexion (mm)	−6.5	1.8	−7.4	0.2	−0.9	0.0	−19.3
Max Plantarflexion (degrees)	−4.1	1.1	−4.7	0.1	−0.6	0.0	−12.3
% of Gait @ Max Plantar-	67.2	5.9	68.4	5.5	1.2	0.0	64.6
Range of Motion (mm)	5.6	1.6	8.8	1.4	3.2	1.0	29.6
Range of Motion (degrees)	3.6	1.0	5.6	0.9	2.0	1.0	18.8
Peak Moment (Nm)	16.3	5.6	19.5	1.5	3.2	1.0	30.2
% of Gait @ Peak Moment	56.7	7.9	51.7	1.5	−5.0	0.0	42.1
Peak Power Out (W)	7.5	2.3	14.2	2.7	6.7	1.0	22.4
% of Gait @ Peak Power	43.9	29.5	53.5	1.3	9.7	0.0	49.6
Power Amplification (ratio)	1.6	0.5	1.9	0.3	0.3	0.0	1.9

“pre” column = mean value on day one; (+/−) Std = standard deviation of previous column; “post” column = mean value on final day; “Delta” column = “post” - “pre;” “t-test” column (alpha =0.01) tests null hypothesis that the “pre” and “post” data come from distributions of equal means (value of 1 = the means are not equal, value of 0 = the means are equal; “Typ Val” column = mean values of an able bodied male subject (76.2 kg) walking with the PAFO at similar speeds.

NIH-PA Author Manuscript

NIH-PA Author Manuscript

Table 3

Subject Two Key Metrics

	pre	(+/−) Std	post	(+/−) Std	Delta	t-test	
cadence (steps/min)	35.2	0.1	39.6	0.1	4.4	1.0	33.1
Max Dorsiflexion (mm)	−2.5	2.4	−3.7	2.2	−1.2	1.0	10.3
Max Dorsiflexion (degrees)	−1.6	1.5	−2.4	1.4	−0.8	1.0	6.6
% of Gait @ Max Dorsi-	36.6	6.7	37.1	2.8	0.5	0.0	39.8
Max Plantarflexion (mm)	−6.4	0.3	−21.0	1.0	−14.6	1.0	−19.3
Max Plantarflexion (degrees)	−4.1	0.2	−13.4	0.6	−9.3	1.0	−12.3
% of Gait @ Max Plantar-	66.4	7.1	66.9	2.0	0.6	0.0	64.6
Range of Motion (mm)	3.9	2.5	17.1	2.8	13.2	1.0	29.6
Range of Motion (degrees)	2.5	1.6	10.9	1.8	8.4	1.0	18.8
Peak Moment (Nm)	31.8	4.1	17.4	2.1	−14.5	1.0	30.2
% of Gait @ Peak Moment	64.9	4.8	51.3	5.8	−13.7	1.0	42.1
Peak Power Out (W)	15.0	3.1	16.3	3.6	1.3	0.0	22.4
% of Gait @ Peak Power	61.2	6.8	56.3	3.1	−4.9	1.0	49.6
Power Amplification (ratio)	0.7	0.2	1.5	0.2	0.8	1.0	1.9

“pre” column = mean value on day one; (+/−) Std = standard deviation of previous column; “post” column = mean value on final day; “Delta” column = “post” - “pre;” “t-test” column (alpha =0.01) tests null hypothesis that the “pre” and “post” data come from distributions of equal means (value of 1 = the means are not equal, value of 0 = the means are equal; “Typ Val” column = mean values of an able bodied male subject (76.2 kg) walking with the PAFO at similar speeds.

NIH-PA Author Manuscript
NIH-PA Author Manuscript

Table 4

Subject Three Key Metrics - Over Ground Data

	pre	(+/−) Std	post	(+/−) Std	Delta	t-test	Typ Val
cadence (steps/min)	34.9	1.7	37.2	1.8	2.3	1.0	33.1
Max Dorsiflexion (mm)	−0.4	2.8	0.1	2.8	0.5	0.0	10.3
Max Dorsiflexion (degrees)	−0.2	1.8	0.1	1.8	0.3	0.0	6.6
% Gait @ Max Dorsi-	45.8	3.7	44.0	2.4	−1.8	1.0	39.8
Max Plantarflexion (mm)	−16.0	0.3	−20.4	1.3	−4.4	1.0	−19.3
Max Plantarflexion (degrees)	−10.2	0.2	−13.0	0.8	−2.8	1.0	−12.3
% of Gait @ Max Plantar-	66.7	3.9	66.0	3.7	−0.7	0.0	64.6
Range of Motion (mm)	15.6	2.9	20.6	2.4	5.0	1.0	29.6
Range of Motion (degrees)	9.9	1.8	13.1	1.5	3.2	1.0	18.8
Peak Moment (Nm)	20.8	4.5	19.1	4.3	−1.6	1.0	30.2
% of Gait @ Peak Moment	52.7	5.0	48.1	2.8	−4.6	1.0	42.1
Peak Power Out (W)	19.0	6.5	17.2	5.7	−1.8	0.0	22.4
% of Gait @ Peak Power	55.4	2.6	52.6	2.9	−2.7	1.0	49.6
Power Amplification (ratio)	1.4	0.2	1.4	0.2	0.0	0.0	1.9

"pre" column = mean value on day one; (+/−) Std = standard deviation of previous column; "post" column = mean value on final day; "Delta" column = "post" -"pre;" "t-test" column (alpha =0.01) tests null hypothesis that the "pre" and "post" data come from distributions of equal means (value of 1 = the means are not equal, value of 0 = the means are equal; "Typ Val" column = mean values of an able bodied male subject (76.2 kg) walking with the PAFO at similar speeds.

NIH-PA Author Manuscript

NIH-PA Author Manuscript

Table 5

Subject Three Key Metrics - Treadmill Data

	pre	(+/−) Std	post	(+/−) Std	Delta	t-test	Typ Val
Cadence in steps/min	29.4	1.4	45.6	1.8	16.2	1.0	33.1
Max Dorsiflexion (mm)	6.1	2.8	11.5	2.0	5.4	1.0	10.3
Max Dorsiflexion (degrees)	3.9	1.8	7.3	1.3	3.4	1.0	6.6
% of Gait @ Max Dorsi-	49.4	2.2	43.4	1.5	−6.0	1.0	39.8
Max Plantarflexion (mm)	−14.7	1.4	−19.2	2.0	−4.5	1.0	−19.3
Max Plantarflexion (degrees)	−9.3	0.9	−12.2	1.3	−2.9	1.0	−12.3
% of Gait @ Max Plantar-	66.1	2.0	67.4	3.0	1.3	1.0	64.6
Range of Motion (mm)	20.8	3.7	30.7	3.0	10.0	1.0	29.6
Range of Motion (degrees)	13.2	2.4	19.5	1.9	6.3	1.0	18.8
Peak Moment (Nm)	29.4	5.1	40.4	3.8	10.9	1.0	30.2
% of Gait @ Peak Moment	51.1	2.3	44.7	1.6	−6.4	1.0	42.1
Peak Power Out (W)	26.6	7.0	50.2	10.6	23.6	1.0	22.4
% of Gait @ Peak Power	54.5	2.3	51.4	4.0	−3.1	1.0	49.6
Power Amplification (ratio)	2.0	0.3	1.5	0.2	−0.5	1.0	1.9

“pre” column = mean value on day one; (+/−) Std = standard deviation of previous column; “post” column = mean value on final day; “Delta” column = “post” - “pre;” “t-test” column (alpha =0.01) tests null hypothesis that the “pre” and “post” data come from distributions of equal means (value of 1 = the means are not equal, value of 0 = the means are equal; “Typ Val” column = mean values of an able bodied male subject (76.2 kg) walking with the PAFO at similar speeds.